Journal of Sound and Vibration (2002) **257**(5), 996–1006
doi:10.1006/jsvi.5032, available online at http://www.idealibrary.com on IDEAL®

CONTINUOUS AND DISCRETE MODELS FOR LONGITUDINALLY VIBRATING ELASTIC RODS VISCOUSLY DAMPED IN-SPAN

Ş. YÜKSEL

Department of Mechanical Engineering, Faculty of Engineering and Architecture, Gazi University, 06570 *Maltepe, Ankara, Turkey. E-mail: yuksel@mmf.gazi.edu.tr*

AND

M. GÜRGÖZE

Faculty of Mechanical Engineering, İstanbul Technical University, 80191 *Gümüşsuyu, İstanbul, Turkey*

(*Received* 11 *December* 2001, *and in final form* 30 *January* 2002)

1. INTRODUCTION

Having the importance of reducing force transmissibility and decreasing displacement, viscously damped elastic structures have received considerable attention. Viscous dampers in the design of vibrating systems such as flexible beams, longitudinal rods and cables are frequently used. The following are some studies on the viscously damped structures in the literature.

Considering the flexural vibrating beams, Zarek and Gibbs [1] derived the complex eigenvalues and mode shapes for a damped beam with general end conditions and presented some sample results. Oliveto *et al*. [2] studied the complex mode superposition method for the dynamic analysis of a simply supported Euler–Bernoulli beam with two rotational viscous dampers attached at its ends. They stated that an appropriate choice of the damper constant allows for the maximum reduction of the dynamic response or for an optimal overall design. Yang and Wu [3] proposed an exact closed-form solution method for transient analysis of general one-dimensional distributed systems subject to arbitrary external, initial and boundary disturbances. They demonstrated the method on a cantilever beam with end mass, viscous damper and spring.

On the other hand, Kovacs [4] studied a taut cable supported with a viscous damper which has application in the design of bridges and other structures. He used a semi-empirical interpolation to obtain the maximum modal damping ratio. Pacheco *et al.* [5] proposed a universal curve relating the modal damping ratio, the mode number, size and location of the damper, and the cable parameters consisting of span, mass and fundamental frequency. They obtained the curve from a numerical complex eigenvalue analysis and illustrated its use for some example situations to find the value of optimal external damping constant. In a recent study, Krenk [6] formulated the problem of damping of a vibrating string by a concentrated viscous damper and solved it by using the complex valued modes. He obtained an asymptotic approximation of the damping ratio of the lower modes which yields a simple analytical formula. In addition to these works related to the cable, Casarella and Laura [7] formulated an analytical expression for the

0022-460X/02/$35.00

viscous drag on a smooth circular cylindrical rodlike cable oscillating with longitudinal and torsional motion. They presented an approximate value for the drag coefficient based on a linear damping law. Furthermore, Goeller and Laura [8] analyzed the dynamic stresses and displacements in a cable subjected to longitudinal excitation simulating ocean-wave motion. They considered the cable to be made up of two segments of different materials and physical dimensions. In their analysis, external damping due to fluid action and internal damping due to viscoelastic material properties were included.

Having a similar equation of motion with that of the cable, the damping of longitudinally vibrating bars can be studied similarly. Singh *et al.* [9] investigated a longitudinally vibrating bar fixed at one end and constrained by a lumped damper with viscous damping coefficient at the other. They developed a closed-form eigensolution. In a different study, Hull [10] considered the same problem with an external axial force. He developed a closed-form series solution for the axial wave equation of this longitudinal vibrating bar with a fixed boundary at one end and a viscously damped one at the other. He also showed that the closed-form solution is more computationally efficient than a finite element solution and the truncation error at lower frequencies is extremely small. Furthermore, Hizal and Gürgöze [11] presented a study dealing with a longitudinally vibrating elastic rod fixed at one end and free at the other, damped viscously by a single damper in-span. They studied the eigencharacteristics of the rod and compared the results regarding the same system first as continuous and then discrete.

In the present paper, the eigencharacteristics of a longitudinally vibrating rod fixed at both ends and damped viscously by a single damper in-span are studied. At first, a continuous model of the rod is considered and the complex eigenfrequencies are presented as the solution of the complex characteristic equation, and moreover, an asymptotic solution is derived to obtain a simple explicit formula for calculating the complex eigenfrequencies and the damping ratio. After that, two different discrete models are formed for the rod in order to determine its eigenvalues which are compared with the complex eigenfrequencies of the continuous model. For the sake of completeness, the studied cases are also considered without damping to see what the effect of a single damper is on the vibrations of the rod.

2. CONTINUOUS MODEL

The mechanical system to be considered is shown in Figure 1. It consists of a longitudinal vibrating elastic rod fixed at both ends and damped viscously in-span. The following expression is the well-known partial differential equation of the rod [12]:

$$EA\frac{\partial^2 u(x,t)}{\partial x^2} = m\frac{\partial^2 u(x,t)}{\partial t^2}, \tag{1}$$

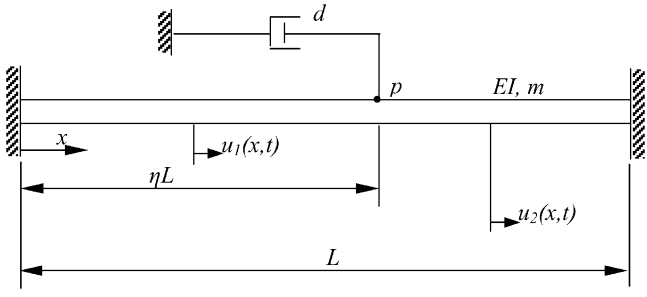

Figure 1. Longitudinally vibrating elastic rod damped viscously in-span: continuous model.

where $u(x,t)$ denotes the axial displacement at a position x, m denotes the mass per unit length of the rod and EA denotes the axial stiffness, in which the E is the modulus of elasticity and A is the cross-sectional area. Dividing the rod into two parts as the left and the right of attachment point of the damper, $u_1(x,t)$ and $u_2(x,t)$ represent the axial displacements of these two sections. These are subject to same differential equation of motion (1) that must be satisfied over the length of the rod.

The equation of motion is to be solved with the boundary and matching conditions;

$$u_1(0,t) = 0, \quad u_2(L,t) = 0,$$

$$u_1(\eta L,t) = u_2(\eta L,t),$$

$$u_1'(\eta L,t) - u_2'(\eta L,t) + \left(\frac{d}{EA}\right)\dot{u}_1(\eta L,t) = 0, \tag{2}$$

where ηL shows the location of the attachment point of the damper and d denotes the damping coefficient. Here, primes and dots refer to partial derivatives with respect to the position coordinate x and time t respectively.

Assuming the axial displacements $u_1(x,t)$ and $u_2(x,t)$ are separable in space and time in the form

$$u_j(x,t) = U_j(x)\mathrm{e}^{\lambda t}, \quad j = 1,2 \tag{3}$$

in which $U_j(x)$ and λ correspond to unknown amplitude function and characteristic value, respectively, one can write the differential equation of the eigenvalue problem as

$$\frac{\mathrm{d}^2 U_j(x)}{\mathrm{d}x^2} - \beta^2 U_j(x) = 0, \quad j = 1,2, \tag{4}$$

where

$$\beta^2 = \frac{m\lambda^2}{EA}. \tag{5}$$

These differential equations have the general solutions

$$U_1(x) = C_1\mathrm{e}^{\beta x} + C_2\mathrm{e}^{-\beta x},$$
$$U_2(x) = C_3\mathrm{e}^{\beta x} + C_4\mathrm{e}^{-\beta x}, \tag{6}$$

where $C_1 - C_4$ are the integration constants to be determined by the boundary and matching conditions given in equation (2). These boundary and matching conditions in connection with the assumed solutions in equation (3) lead to the four equations in the four unknown coefficients $C_1 - C_4$. Writing these as a single-matrix equation and equating the determinant of the coefficients to zero result in the characteristic equation

$$2\sinh\bar{\beta} + a[\cosh\bar{\beta} - \cosh(1-2\eta)\bar{\beta}] = 0, \tag{7}$$

where the notations

$$\bar{\beta} = \beta L, \quad a = \frac{d\lambda}{EA\beta} = \frac{d}{\sqrt{EAm}} \tag{8}$$

are introduced for simplicity and a can be considered as the dimensionless damping coefficient.

This characteristic equation is very similar to that of reference [11]. Therefore, it can be solved to determine the complex frequencies $\bar{\beta}$ by using the same approach in that reference. Considering the $\bar{\beta}$ as a complex number, the equation (7) can be written in the

form of two real equations after lengthy calculations as

$$(2\sinh x + a\cosh x)\cos y - a\cosh(1-2\eta)x\cos(1-2\eta)y = 0, \tag{9}$$

$$(2\cosh x + a\sinh x)\sin y - a\sinh(1-2\eta)x\sin(1-2\eta)y = 0, \tag{10}$$

where x denotes the real part and y denotes the imaginary part of the $\bar{\beta}$. These two equations are to be solved simultaneously.

Besides, an asymptotic solution of the characteristic equation can be obtained by applying a small perturbation on the solution without damping, similar to the solution technique in reference [6].

3. ASYMPTOTIC SOLUTION

In this part of the paper, finding an asymptotic solution is the first concern in order to gain as much insight into the system behavior as possible. Here, the characteristic parameter $\bar{\beta}$ is used in the form of complex number. Then, the complex frequencies of the undamped longitudinally vibrating rod fixed at both ends are

$$\bar{\beta}_n^0 = \mathrm{i}n\pi, \quad n = 1, \ldots, \infty. \tag{11}$$

Now, one can assume a small perturbation as $\Delta \ll 1$ between the complex frequencies of the damped and undamped cases

$$\bar{\beta}_n - \bar{\beta}_n^0 = \Delta, \quad n = 1, \ldots, \infty. \tag{12}$$

Utilizing this assumption in the characteristic equation given in equation (7) leads to the following explicit expression for the characteristic parameters $\bar{\beta}_n$ after lengthy calculations

$$\bar{\beta}_n \cong \mathrm{i}n\pi - a\sin^2 \eta n\pi, \quad n = 1, \ldots, \infty. \tag{13}$$

The well-known representation of the characteristic value λ with the real and imaginary parts is

$$\lambda = -\zeta\omega_n \pm \mathrm{i}\sqrt{1-\zeta^2}\omega_n, \tag{14}$$

where $\mathrm{i} = \sqrt{-1}$ and ω_n denotes the undamped natural frequency, and ζ denotes the damping ratio that can be evaluated by using the real and imaginary parts of the characteristic value as [12]

$$\zeta = \frac{|\mathrm{Re}(\lambda)|}{\sqrt{|\mathrm{Re}(\lambda)|^2 + |\mathrm{Im}(\lambda)|^2}}. \tag{15}$$

Hence, in this study, the asymptotic approximation of the damping ratio can be expressed as

$$\zeta_n \cong \frac{a\sin^2 \eta n\pi}{\sqrt{(n\pi)^2 + (a\sin^2 \eta n\pi)^2}}, \quad n = 1, \ldots, \infty. \tag{16}$$

Furthermore, because of its convenience for practical applications in which $\eta \ll 1$, equation (13) takes the form

$$\bar{\beta}_n \cong \mathrm{i}n\pi - a(\eta n\pi)^2, \quad n = 1, \ldots, \infty \tag{17}$$

and equation (16) leads to

$$\zeta_n \cong \frac{an\pi\eta^2}{\sqrt{1+(an\pi)^2\eta^4}}, \quad n = 1, \ldots, \infty \tag{18}$$

and takes the final form

$$\zeta_n \cong n\pi a\eta^2, \quad n = 1, \ldots, \infty. \tag{19}$$

A similar expression was given in reference [5] for a taut cable with similar boundary conditions and a single damper close to support.

Note that neither equation (16) nor (19) gives a peak value for the dimensionless damping coefficient a. Instead, there is a linear relation between the damping ratio ζ and the coefficient a for a given attachment point location of the damper η. In fact, this result is expected for small damping coefficients. On the other hand, an optimal value for the damping ratio for a given damper location can be calculated by solving the two simultaneous equations numerically, but for large damping coefficients.

4. DISCRETE MODEL

An equivalent discrete model to the original continuous system model which is depicted in Figure 1 can be obtained by dividing the rod into equal segments as shown in Figure 2. The new model consists of n equal masses M connected by the springs of equivalent stiffnesses k and $2k$, where k is such that the springs undergo the same elongations as the corresponding rod segments under identical segments. Furthermore, the system is viscously damped on the pth mass.

The equation of motion of the discrete model can be written in the form of

$$\mathbf{M}\ddot{\mathbf{x}} + \mathbf{C}\dot{\mathbf{x}} + \mathbf{K}\mathbf{x} = \mathbf{0}, \tag{20}$$

where $\mathbf{M}$, $\mathbf{C}$ and $\mathbf{K}$ denote the mass, damping and stiffness matrices respectively. The mass and damping matrices are same with those of reference [11]. The only differences are in the values of the (1, 1) and (n, n)th elements of the stiffness matrix. The values of the elements are 3 in this study instead of 2 and 1 in that reference.

Now, equation (20) can be transformed to a set of first order differential equations by using the so-called $(2n \times 2n)$ state matrix which is in the same form of that in reference [11]. The eigenvalues of the state matrix are to be determined as complex numbers. Then, one can make a comparison between the resulting complex numbers multiplied by L/c where c is the velocity of the wave propagation along the rod and the complex frequencies $\bar{\beta}$ of the continuous model.

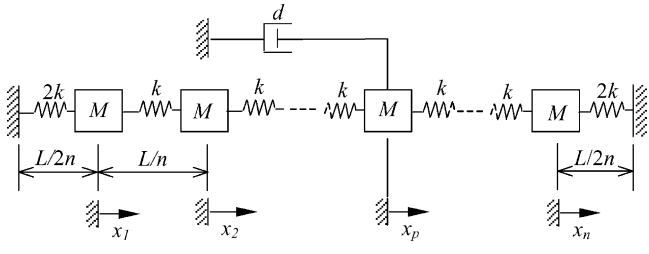

Figure 2. Longitudinally vibrating elastic rod damped viscously in-span: discrete model: first type.

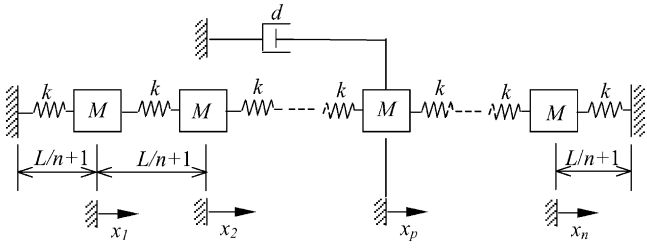

Figure 3. Longitudinally vibrating elastic rod damped viscously in-span: discrete model: second type.

On the other hand, one can consider the discrete model as shown in Figure 3 instead of the model in Figure 2. The difference between these two models is that the springs at the right and left ends in Figure 2 are stiffer but shorter than the springs at the ends in Figure 3. In this case, the equation of motion of the new model has the same mass and damping matrices, the stiffness matrix is the same except the multiplier k takes the following form

$$k = (n+1)\frac{EA}{L}, \tag{21}$$

which is different than that of the first model. Additionally, both the (1, 1) and (n, n)th elements of the stiffness matrix take the same value 2. Similar to the preceding procedure, one can transform the equation of motion to a set of first order differential equations by using the state matrix which is in the same form, solve for the eigenvalues as complex numbers, and compare with the complex frequencies of the continuous model.

5. NUMERICAL SOLUTIONS

In this section, the numerical solutions of the expression for the continuous and discrete models are presented. It is assumed that the rod material is aluminum for which the density is $\rho = 2860\,\mathrm{kg/m^3}$ and the modulus of elasticity is $E = 7 \times 10^{10}\,\mathrm{N/m^2}$. For the rod geometry, the values of the cross-sectional area $A = 3{\cdot}14 \times 10^{-4}\,\mathrm{m^2}$ and the length of the rod $L = 1\,\mathrm{m}$ are used. To complete the numerical values needed, the damping coefficient $d = 100\,\mathrm{N\,s/m}$ is also used.

Concerning the undamped case first, Table 1 presents the eigenfrequencies of the models. The first row contains the analytical solution. The following rows consist of two columns: One column presents the eigenfrequencies of the discrete model shown in Figure 2 while the other presents the those of the model in Figure 3, depending on the number of degrees of freedom n. It can be seen from the values in the table that modelling the longitudinally vibrating rod as shown in Figure 2 gives a better approximation to the results of the analytical solution for the eigenfrequencies than the modelling as in Figure 3. Also, increasing the selected degrees of freedom decreases the approximation error.

In order to see the effect of the single damper in-span on the eigencharacteristics of the longitudinally vibrating rod, Table 2 presents the complex eigenfrequencies of the damped case in which the location of the attachment point $\eta = 0{\cdot}6$ which is used is similar to that in reference [11]. The first row shows the results of the simultaneous solution of the two real equations given in equations (9) and (10), derived from the complex characteristic equation of the continuous model. The other rows present the eigenvalues of the state matrix. Depending on the number of equal masses in the discrete models shown in Figures 2 and 3, the results are multiplied by L/c in order to compare with the complex

TABLE 1

First four dimensionless eigenfrequencies of the un-damped rod

	ω_1		ω_2		ω_3		ω_4	
	3·141593		6·283185		9·424778		12·566371	
n	Figure 2	Figure 3	Figure 2	Figure 3	Figure 2	Figure 3	Figure 2	Figure 3
1	1·732050	2						
2	2·828427	2·449490	4·000000	4·242641				
3	3·000000	2·651309	5·196152	4·898979	6·000000	6·400825		
4	3·061467	2·763932	5·656854	5·257311	7·391036	7·236068	8·000000	8·506508
5	3·090169	2·835221	5·877852	5·477225	9·510565	7·745966	10·000000	9·486833
10	3·128689	2·985221	6·180339	5·909672	9·079809	8·713819	11·755705	11·340577
50	3·141075	3·110148	6·279051	6·217347	9·410831	9·318647	12·533323	12·411109
100	3·141463	3·125875	6·282151	6·250995	9·421290	9·374602	12·558103	12·495942
500	3·141587	3·138451	6·283143	6·276870	9·424638	9·415228	12·566039	12·553494
1000	3·141591	3·140022	6·283174	6·280036	9·424743	9·420034	12·566287	12·560009
1500	3·141592	3·140545	6·283180	6·281087	9·424762	9·421622	12·566333	12·562147

eigenfrequencies of the continuous model given in the first row. The results make clear that the increasing number of discrete masses causes a decreased approximation error as expected. It is also noticeable that using the model in Figure 2 gives better approximation than using the model in Figure 3.

Figure 4 presents the real and imaginary parts of the complex eigencharacteristics $\bar{\beta}_n$ for the certain range of the damped model given in Figure 2. This illustrates the nature of the convergence with n. In Figure 4(a), it can be seen that the discrete mass approximation underestimates the real part of the eigencharacteristics for the first and third modes but overestimates for the second and fourth modes. In Figure 4(b), on the other hand, the discrete mass approximation underestimates the imaginary parts for all four modes. For the discrete model depicted in Figure 3, very similar curves can be plotted and shows the same nature of convergence with n.

On the other hand, the two simultaneous equations given in equations (9) and (10) can be solved with the help of MATLAB to obtain the exact values for the complex eigenfrequencies. Using the results, Figure 5 illustrates the dimensionless damping values with respect to the dimensionless damping coefficients for the given locations $\eta = 0{\cdot}05$ and $0{\cdot}02$ of attachment point of the damper. Similar curves are given in references [4–6] for a taut cable with similar end conditions and a single damper close to the support and called "universal curves". It is seen from Figure 5 that increasing the damping coefficient does not result in a better damping ratio; instead, there is a peak value of the damping, called the optimal value. The optimal values can also be calculated from the results of the numerical solution with the help of MATLAB. The exact optimal values are

$$a\eta|_{opt} = 0{\cdot}315, \quad \left.\frac{\zeta}{\eta}\right|_{opt} = 0{\cdot}529 \quad \text{for } \eta = 0{\cdot}05,$$

$$a\eta|_{opt} = 0{\cdot}319, \quad \left.\frac{\zeta}{\eta}\right|_{opt} = 0{\cdot}511 \quad \text{for } \eta = 0{\cdot}02.$$

By analogy with the taut cable problem, these exact optimal values are very close to the approximate optimal values in the references mentioned above.

TABLE 2

First four dimensionless eigenfrequencies of the damped rod

	$\bar{\beta}_1$		$\bar{\beta}_2$		$\bar{\beta}_3$		$\bar{\beta}_4$	
	$-0{\cdot}020349 + 3{\cdot}141619i$		$-0{\cdot}007772 + 6{\cdot}283168i$		$-0{\cdot}007772 + 9{\cdot}424794i$		$-0{\cdot}020349 + 12{\cdot}566343i$	
n	Figure 2	Figure 3	Figure 2	Figure 3	Figure 2	Figure 3	Figure 2	Figure 3
1	$-0{\cdot}011248 + 1{\cdot}732014i$	$-0{\cdot}011248 + 1{\cdot}414169i$						
2	$-0{\cdot}011249 + 1{\cdot}732014i$	$-0{\cdot}011249 + 2{\cdot}000032i$	$-0{\cdot}011247 + 3{\cdot}999857i$	$-0{\cdot}011248 + 3{\cdot}463974i$				
3	$-0{\cdot}022497 + 2{\cdot}999971i$	$-0{\cdot}016873 + 2{\cdot}296090i$	$-0{\cdot}000000 + 5{\cdot}196152i$	$-0{\cdot}000000 + 4{\cdot}242641i$	$-0{\cdot}011247 + 5{\cdot}999876i$	$-0{\cdot}016872 + 5{\cdot}543128i$		
4	$-0{\cdot}019203 + 3{\cdot}061498i$	$-0{\cdot}016279 + 2{\cdot}472153i$	$-0{\cdot}011248 + 5{\cdot}656798i$	$-0{\cdot}006218 + 4{\cdot}702263i$	$-0{\cdot}003294 + 7{\cdot}391049i$	$-0{\cdot}006218 + 6{\cdot}472153i$	$-0{\cdot}011246 + 7{\cdot}999802i$	$-0{\cdot}016278 + 7{\cdot}608218i$
5	$-0{\cdot}022497 + 3{\cdot}090161i$	$-0{\cdot}018748 + 2{\cdot}588186i$	$-0{\cdot}000000 + 5{\cdot}877852i$	$-0{\cdot}000000 + 5{\cdot}000000i$	$-0{\cdot}022498 + 8{\cdot}090110i$	$-0{\cdot}018749 + 7{\cdot}071043i$	$-0{\cdot}000000 + 9{\cdot}510565i$	$-0{\cdot}000000 + 8{\cdot}660254i$
10	$-0{\cdot}021947 + 3{\cdot}128695i$	$-0{\cdot}020038 + 2{\cdot}846301i$	$-0{\cdot}002148 + 6{\cdot}180338i$	$-0{\cdot}001623 + 5{\cdot}634650i$	$-0{\cdot}017861 + 9{\cdot}079823i$	$-0{\cdot}016923 + 8{\cdot}308311i$	$-0{\cdot}007772 + 11{\cdot}755693i$	$-0{\cdot}005978 + 10{\cdot}812809i$
50	$-0{\cdot}020746 + 3{\cdot}141098i$	$-0{\cdot}020405 + 3{\cdot}079527i$	$-0{\cdot}006459 + 6{\cdot}279040i$	$-0{\cdot}006112 + 6{\cdot}156080i$	$-0{\cdot}009838 + 9{\cdot}410885i$	$-0{\cdot}010011 + 9{\cdot}226856i$	$-0{\cdot}018419 + 12{\cdot}533294i$	$-0{\cdot}017674 + 12{\cdot}288801i$
100	$-0{\cdot}020552 + 3{\cdot}141488i$	$-0{\cdot}020386 + 3{\cdot}110386i$	$-0{\cdot}007107 + 6{\cdot}282133i$	$-0{\cdot}006915 + 6{\cdot}219959i$	$-0{\cdot}008794 + 9{\cdot}422130i$	$-0{\cdot}008901 + 9{\cdot}328097i$	$-0{\cdot}019448 + 12{\cdot}558075i$	$-0{\cdot}019074 + 12{\cdot}433899i$
500	$-0{\cdot}020390 + 3{\cdot}141613i$	$-0{\cdot}020358 + 3{\cdot}135343i$	$-0{\cdot}007638 + 6{\cdot}283127i$	$-0{\cdot}007597 + 6{\cdot}270587i$	$-0{\cdot}007974 + 9{\cdot}424655i$	$-0{\cdot}007999 + 9{\cdot}405844i$	$-0{\cdot}020180 + 12{\cdot}566012i$	$-0{\cdot}020106 + 12{\cdot}540932i$
1000	$-0{\cdot}020370 + 3{\cdot}141618i$	$-0{\cdot}020354 + 3{\cdot}138479i$	$-0{\cdot}007705 + 6{\cdot}283158i$	$-0{\cdot}007684 + 6{\cdot}276882i$	$-0{\cdot}007873 + 9{\cdot}424759i$	$-0{\cdot}007886 + 9{\cdot}415345i$	$-0{\cdot}020265 + 12{\cdot}566260i$	$-0{\cdot}020229 + 12{\cdot}553707i$
1500	$-0{\cdot}020363 + 3{\cdot}141618i$	$-0{\cdot}020405 + 3{\cdot}139527i$	$-0{\cdot}007727 + 6{\cdot}283164i$	$-0{\cdot}007701 + 6{\cdot}280012i$	$-0{\cdot}007839 + 9{\cdot}424779i$	$-0{\cdot}007854 + 9{\cdot}417654i$	$-0{\cdot}020293 + 12{\cdot}566306i$	$-0{\cdot}020289 + 12{\cdot}557809i$

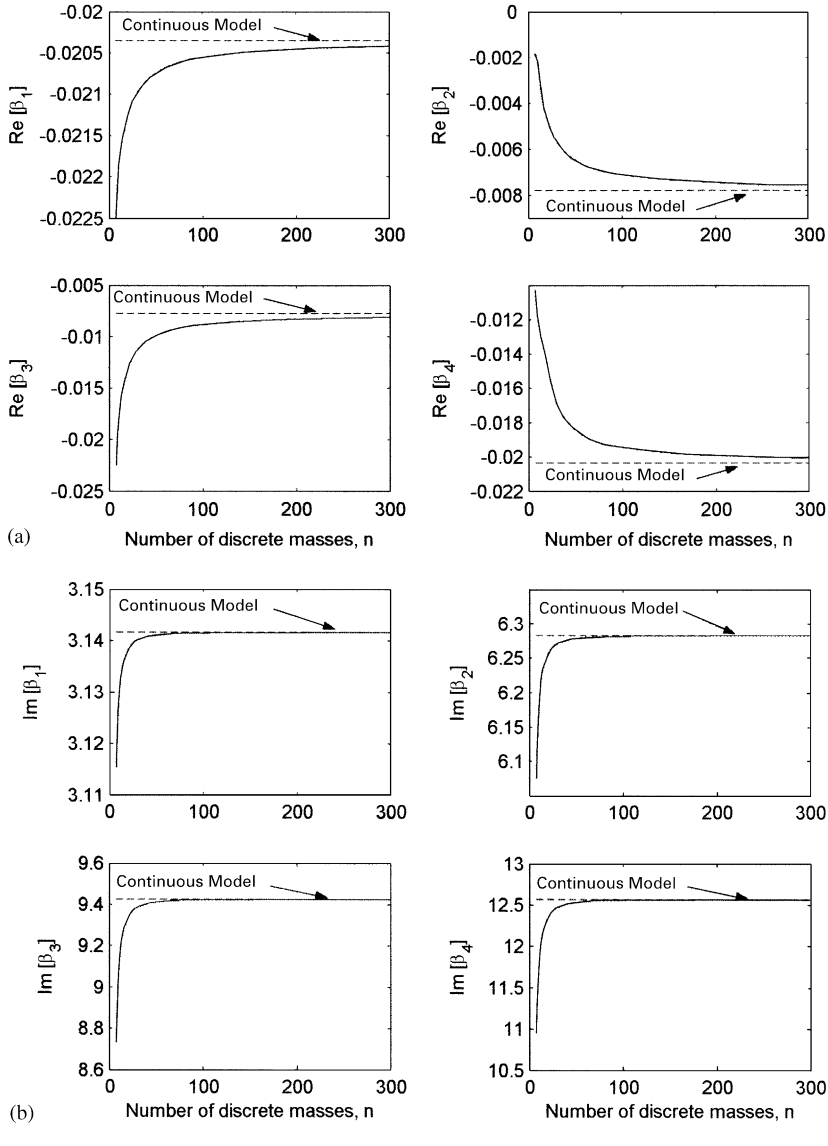

Figure 4. Convergence of (a) the real parts and (b) the imaginary parts of the eigencharacteristics $\bar{\beta}_n$ with the degrees of freedom n.

6. CONCLUSIONS

In this study, continuous and two different discrete models of a longitudinally vibrating elastic rod fixed at both ends are investigated. The rod is damped viscously by a single damper in-span. The expressions are derived and solved numerically for the eigenfrequencies of the continuous and discrete models. An asymptotic solution is also utilized to derive a single explicit formula for both the complex frequencies and the damping ratio. In order to make a comparison for the effect of the damper, the eigenfrequencies of the rod without damping are obtained similarly by utilizing a continuous and also two different discrete models. The corresponding numerical results are presented in tables and plots.

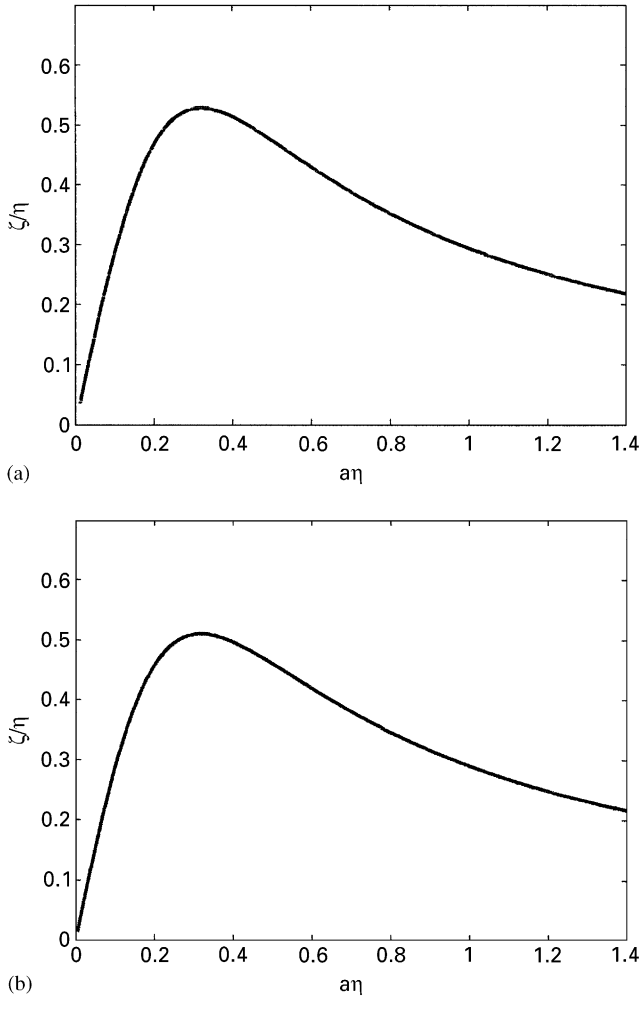

Figure 5. Damping ratios for (a) $\eta = 0{\cdot}05$ and (b) $\eta = 0{\cdot}02$.

REFERENCES

1. J. H. Zarek and B. M. Gibbs 1981 *Journal of Sound and Vibration* **78**, 185–196. The derivation of eigenvalues and mode shapes for the bending motion of a damped beam with general end conditions.
2. G. Oliveto, A. Santini and E. Tripodi 1997 *Journal of Sound and Vibration* **200**, 327–345. Complex modal analysis of a flexural vibrating beam with viscous end conditions.
3. B. Yang and X. Wu 1997 *Journal of Sound and Vibration* **208**, 763–776. Transient response of one dimensional distributed systems: a closed form eigenfunction expansion realization.
4. I. Kovacs 1982 *Die Bautechnik* **59**, 325–332. Zur Frage der Seilschwigungen und der Seildampfung.
5. B. N. Pacheco, Y. Fujino and A. Sulekh 1993 *Journal of Structural Engineering* **119**, 1961–1979. Estimation curve for modal damping in stay cables with viscous damper.
6. S. Krenk 2000 *Journal of Applied Mechanics* **67**, 772–776. Vibrations of a taut cable with an external damper.
7. M. J. Casarella and P. A. Laura 1969 *Journal of Hydronautics* **3**, 180–183. Drag on an oscillating rod with longitudinal and torsional motion.

8. J. E. Goeller and P. A. Laura 1969 *The Journal of the Acoustical Society of America* **46** (Part 1), 284–292. Dynamic stress and displacements in a two-material cable system subjected to longitudinal excitation.
9. R. Singh, W. M. Lyons and G. Prater 1989 *Journal of Sound and Vibration* **133**, 364–367. Complex eigensolution for longitudinally vibrating bars with a viscously damped boundary.
10. A. J. Hull 1994 *Journal of Sound and Vibration* **169**, 19–28. A closed form solution of a longitudinal bar with a viscous boundary condition.
11. N. A. Hizal, M. Gürgöze 1998 *Journal of Sound and Vibration* **216**, 328–336. Lumped parameter representation of a longitudinally vibrating elastic rod viscously damped in-span.
12. D. J. Inman 2001 *Engineering Vibration.* Englewood Cliffs, NJ: Prentice-Hall.